

A Bose gas in a single-beam optical dipole trap

Lena Simon and Walter T. Strunz

Institut für Theoretische Physik, Technische Universität Dresden, D-01062 Dresden, Germany

(Dated: November 3, 2018)

We study an ultracold Bose gas in an optical dipole trap consisting of one single focused laser beam. An analytical expression for the corresponding density of states beyond the usual harmonic approximation is obtained. We are thus able to discuss the existence of a critical temperature for Bose-Einstein condensation and find that the phase transition must be enabled by a cutoff near the threshold. Moreover, we study the dynamics of evaporative cooling and observe significant deviations from the findings for the well-established harmonic approximation. Furthermore, we investigate Bose-Einstein condensates in such a trap in Thomas-Fermi approximation and determine analytical expressions for chemical potential, internal energy and Thomas-Fermi radii beyond the usual harmonic approximation.

PACS numbers: 05.30.Jp, 37.10.De, 03.75.Hh, 51.10.+y

I. INTRODUCTION

Since the first observation of Bose-Einstein condensation in dilute atomic vapors in a remarkable series of experiments [1, 2, 3], ultracold quantum gases represent an immensely active field of research for experimental scientists and theorists alike. These systems offer an unprecedented variety of possibilities to manipulate and investigate many-body quantum phenomena [4, 5, 6].

A common approach to reach the Bose-Einstein condensation phase transition involves laser cooling of the atomic vapor after which atoms in weak-field seeking states are transferred into a magnetic trap [7, 8], followed by evaporative cooling. While for magnetic traps the potential depends on the magnetic substate of the atoms, optical dipole traps have been used to store atoms independently of their magnetic substate. To give a recent example, Bose-Einstein condensation of Strontium has been achieved in crossed laser beams [9, 10].

A focused laser beam provides an almost perfect realization of a conservative trapping potential for neutral atoms [11], and is the basis for the growing field of ultracold gases in optical lattices [12]. The first attempts to obtain quantum degeneracy in an optical dipole trap were made by Chu et. al. [13], who employed two crossed laser beams. Multiple implementations of optical and evaporative cooling techniques may be used, which allow phase space densities close to quantum degeneracy [14, 15, 16]. Chapman et al. managed to condense ^{87}Rb in a dipole trap consisting of two crossed CO_2 -laser beams by means of evaporative cooling [17] and all-optical crossed-beam setups have also enabled the first observation of Bose-Einstein condensation of Cesium and Ytterbium atoms [18, 19]. Optical traps consisting of one single focused laser beam were used to produce degenerate Fermi gases [20], Fermi gas mixtures [21], to achieve condensation of ^{87}Rb [22], and they are a popular way to trap and store cold gases for multiple needs [23, 24, 25, 26, 27, 28].

Usually the potential of such an optical trap is approximated harmonically for low average temperatures of the atoms compared to the trap depth [20, 21]. For some ap-

plications, however, e.g. for evaporative cooling, typical temperatures need not be that low. Our work is motivated by an experiment of Helm and coworkers [23] who use a single focused CO_2 -laser beam to cool and store an ultracold cloud of ^{87}Rb -atoms. We aim at a more detailed understanding of the evaporation dynamics and of the properties of the ultracold gas in a single-beam trap. Crucially, our analysis is based on the true dipole trap potential without invoking the usual harmonic approximation.

Our article is organized as follows. In section II we manage to derive the density of states of the dipole trap based on the usual semiclassical expression without invoking further approximations. For low energies we recover the well-known expression for the harmonically approximated potential; for energies near threshold, however, we uncover a singularity. Subsequently, we will discuss the critical temperature for Bose-Einstein condensation in such a trap in section III. Remarkably, without further thought the singularity in the density of states prevents Bose-Einstein condensation from occurring. However, a cutoff – most likely introduced by gravity – removes this singularity and paves the way for Bose-Einstein condensation. In section IV the influence of the modified density of states on evaporative cooling will be studied and significant differences to the usual harmonic approximation will be revealed. Finally, in section V we investigate the condensate wave function in Thomas-Fermi approximation in such single-beam optical dipole traps. We conclude with final remarks in section VI.

II. DENSITY OF STATES

We discuss an optical dipole trap consisting of a single focused Gaussian far detuned laser beam. The potential that affects atoms in such a trap is given by [29]

$$U_{\text{dip}}(\rho, z) = -\frac{U_0}{(1 + z^2/z_0^2)} \exp\left(\frac{-2\rho^2}{w_0^2(1 + z^2/z_0^2)}\right) \quad (1)$$

which displays an azimuthal symmetry along the propagation (z -) axis. The energy $U_0 > 0$ is the maximum depth of the trap at $\rho = 0, z = 0$. Here, z_0 denotes the so called Rayleigh length and w_0 the beam waist of the laser which is connected to the laser wave length through $w_0 = \sqrt{\lambda z_0 / \pi}$.

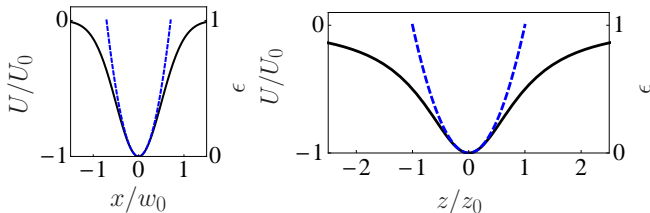


FIG. 1: Dipole trap potential (black, solid) and its harmonic approximation (blue, dashed), at $z = y = 0$ (left) and $x = y = 0$ (right).

If the average thermal energy $k_B T$ of the atoms in the trap is much lower than U_0 , the potential can be approximated harmonically which leads to the expression

$$U_{\text{ha}}(\rho, z) = U_0 \left(-1 + \frac{2\rho^2}{w_0^2} + \frac{z^2}{z_0^2} \right). \quad (2)$$

This harmonic approximation is usually employed to describe cold atoms in dipole traps [20, 21].

For a proper discussion of the thermodynamic properties of a Bose gas we aim at the true density of states $g(E)$ [4] of the dipole trap; the number of single-particle eigenstates between E and $E + dE$ is then given by $g(E)dE$. In the usual semiclassical approximation the phase space is divided into Planck cells of size $(2\pi\hbar)^3$ such that the density of states becomes

$$\begin{aligned} g(E) &= \frac{1}{(2\pi\hbar)^3} \int d^3r d^3p \delta \left(E - U(\mathbf{r}) - \frac{\mathbf{p}^2}{2m} \right) \quad (3) \\ &= \frac{2\pi(2m)^{3/2}}{(2\pi\hbar)^3} \int_{U(\mathbf{r}) \leq E} d^3r \sqrt{E - U(\mathbf{r})}. \end{aligned}$$

In the following it turns out to be convenient to work with a scaled energy (which is zero at the trap center and one at the threshold) and the accompanying scaled density of states:

$$\epsilon = \frac{E + U_0}{U_0}; \quad g(\epsilon) = U_0 g(E), \quad (4)$$

such that $g(\epsilon)d\epsilon = g(E)dE$.

Remarkably, inserting the full dipole trap potential (1) in the semiclassical formula (3) allows us to express the density of states in terms of known special functions. We find

$$\begin{aligned} g_{\text{dip}}(\epsilon) &= G \cdot \sqrt{\epsilon} \left\{ 5F \left(\arctan \left(\sqrt{\frac{\epsilon}{1-\epsilon}} \right), \frac{1}{\epsilon} \right) \right. \\ &\quad \left. - \left(11 - \frac{1}{1-\epsilon} \right) E \left(\arctan \left(\sqrt{\frac{\epsilon}{1-\epsilon}} \right), \frac{1}{\epsilon} \right) \right\}. \quad (5) \end{aligned}$$

Here, $G = \frac{4\pi^2(2mU_0)^{3/2}}{9(2\pi\hbar)^3} z_0 w_0^2$ is a dimensionless constant (see below for a more convenient expression) and $F(\phi, m)$ and $E(\phi, m)$ denote the elliptic integrals [30] of the first and second kind, respectively, with

$$\begin{aligned} F(\phi, m) &= \int_0^\phi (1 - m \sin^2 \theta)^{-1/2} d\theta \\ E(\phi, m) &= \int_0^\phi (1 - m \sin^2 \theta)^{1/2} d\theta \\ &\text{for } -\pi/2 < \phi < \pi/2. \end{aligned}$$

Expanding expression (5) up to second order for small energies leads to the well-known density of states of the harmonic oscillator potential (2), as expected. We find

$$\lim_{\epsilon \rightarrow 0} g_{\text{dip}}(\epsilon) = g_{\text{ha}}(\epsilon) = G \cdot \frac{9\pi}{16} \epsilon^2 = \frac{U_0^3}{2(\hbar\bar{\omega})^3} \epsilon^2, \quad (6)$$

with the geometric mean $\bar{\omega}$ of the trap frequencies derived from the harmonic approximation (2). Thus, the prefactor in (5) can also be written as $G = \frac{8}{9\pi} \frac{U_0^3}{(\hbar\bar{\omega})^3}$ which is typically a large number. The harmonic approximation (6) agrees fairly well with the true density of states of the dipole trap potential $g_{\text{dip}}(\epsilon)$ for energies ϵ up to about one third of the potential depth as can be seen in Figure 2. Clearly, for larger energies the two density of states differ significantly. Expression (5) displays a $\frac{1}{1-\epsilon}$ -singularity (and an additional logarithmic singularity from $F(\phi, m)$) as $\epsilon \rightarrow 1$. As a simple interpolating formula we found

$$g_{\text{dip}}(\epsilon) \approx G \left(\frac{9\pi}{16} \epsilon^2 + \frac{\epsilon^{5/2}}{1-\epsilon} \right), \quad (7)$$

which has correct limits as $\epsilon \rightarrow 0$ and $\epsilon \rightarrow 1$ (see Fig. 2).

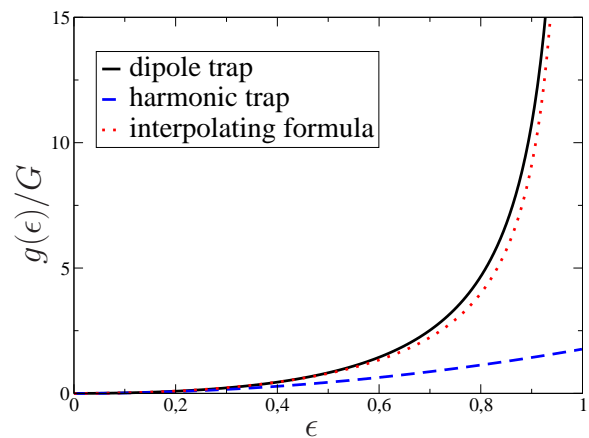


FIG. 2: Comparison of the densities of states of the dipole trap potential (black, solid line) and its harmonic approximation (blue, dashed line), along with the simple approximate formula (7) (dotted line).

The singularity at the potential edge has profound implications for the thermodynamic properties of a Bose gas

in this trap. In particular, we next want to investigate its influence on the critical temperature T_C for Bose-Einstein condensation.

III. CRITICAL TEMPERATURE

Bose-Einstein condensation occurs once the total number of atoms exceeds the maximum possible number of atoms in excited states which is set by the Bose distribu-

tion $f(\epsilon)$ with zero chemical potential. In other words, using our scaled units, the critical temperature for Bose-Einstein condensation for a given total atom number N in the trap is here determined by [31],

$$N = \int_0^1 d\epsilon g(\epsilon) (\exp(\epsilon U_0/k_B T_C) - 1)^{-1}. \quad (8)$$

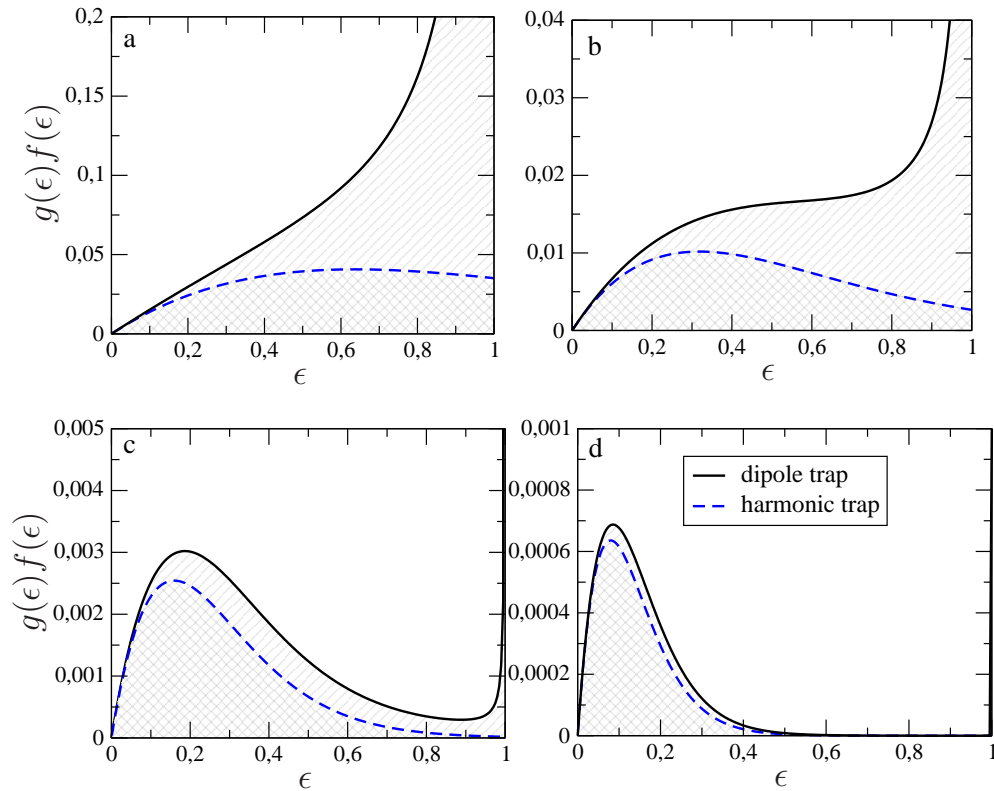


FIG. 3: Comparison of the number density $g(\epsilon)f(\epsilon)$ of the dipole trap potential (black, solid line) and its harmonic approximation (blue, dashed line) for $\eta = U_0/k_B T = 2.5, 5, 10, 20$. The areas below the graphs must be finite to allow for Bose-Einstein condensation.

In case the integral diverges there is no Bose-Einstein condensation as for the well-known case of the one-dimensional harmonic oscillator or the two-dimensional box potential. Figure 3 shows the integrand $g(\epsilon)f(\epsilon)$ of expression (8) with the Bose distribution $f(\epsilon) = (\exp(\eta\epsilon) - 1)^{-1}$ for different ratios $\eta = U_0/k_B T$ of trap depth to thermal energy.

The figure reveals that the number density $g(\epsilon)f(\epsilon)$ diverges for the dipole trap near the potential edge while it stays finite for its harmonic approximation. Well below the singularity, i.e. for small energies, the agreement between the two improves for increasing η , i.e. for lower

temperatures: then the atoms are closer to the trap minimum, where the potential is well characterized by the harmonic approximation. For higher temperatures the atoms populate states of higher energy, where the harmonic potential differs significantly from the dipole trap. For $\epsilon \rightarrow 1$, the product $g(\epsilon)f(\epsilon)$ keeps the singularity from the density of states and it turns out that it is not integrable.

We have to conclude that – strictly speaking – the Bose Einstein phase transition does not occur in a single-beam optical dipole trap, no matter how cold the gas; which contradicts findings of recent experiments [22].

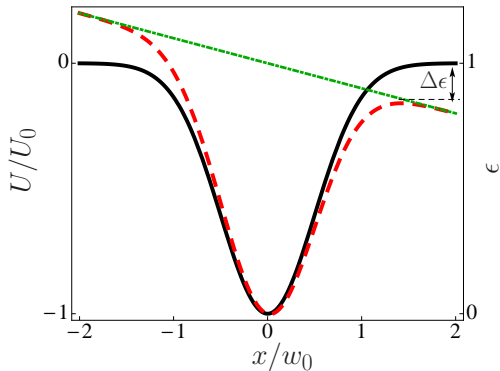


FIG. 4: The dipole trap potential without gravity (black, solid), including gravity (red, dashed), and the pure gravitational potential (green, dashed-dotted) at $y = z = 0$. Due to gravity, atoms may escape from the trap as soon as their energy is $\epsilon > 1 - \Delta\epsilon$. Thus, the real potential is cut off at $\epsilon_t = 1 - \Delta\epsilon$.

In order to shed light on this curious result we have to look at the true experimental conditions in more detail. A solution of this apparent contradiction can be found in gravity – which we neglected up to now. Including gravity, the true potential reads

$$U_{\text{dip}+g}(\vec{r}) = -\frac{U_0}{(1+z^2/z_0^2)} \exp\left(\frac{-2(x^2+y^2)}{w_0^2(1+z^2/z_0^2)}\right) - mgx. \quad (9)$$

As displayed in Figure 4, gravity lowers the threshold energy ϵ_t an atom needs to escape the trap in one spatial direction. Based on the assumption of sufficient ergodicity, we simply assume that gravity effectively leads to a cutoff at a certain scaled energy $\epsilon_t = 1 - \Delta\epsilon$. The cutoff parameter $\Delta\epsilon$ depends on the absolute trap depth U_0 and on the mass of the atoms.

As a consequence of this cutoff, the integral over the number density in equation (8) extends up to $\epsilon_t = 1 - \Delta\epsilon$ only. The integral remains finite and Bose condensation may take place.

In fact, the critical temperature for a given number of atoms can then well be estimated as usual within the harmonic approximation. To give an example, in an optical dipole trap with $U_0 = 200\mu\text{K}$, the critical temperature for 10^5 ^{87}Rb -atoms is approximately 800nK, which is in accordance with $\eta \approx 250$. This implies that the atoms are trapped so deeply that the harmonic approximation is clearly valid – see Figure 1. The same conclusion can be drawn from Figures 3: while for fairly high temperatures ($\eta = 2.5, 5$) the number density in the dipole trap differs

from the harmonic approximation over the whole range of energies, this ceases to be true for low temperatures ($\eta = 20$): here the only difference is the sharp singularity near threshold ($\epsilon \approx 1$) which, as we have argued, turns out to be irrelevant due to gravity.

IV. EVAPORATIVE COOLING

In the last section we came to the conclusion that even though the integral (8) is not integrable in the usual limits, a critical temperature for Bose-Einstein condensation exists due to gravity or any other interaction that effectively cuts off or blurs the singularity as $\epsilon \rightarrow 1$. The harmonic approximation of the potential is sufficient to determine T_c because temperatures are typically low enough. However, for processes involving higher temperatures, as for instance evaporation dynamics, the number density $g(\epsilon)f(\epsilon)$ in the dipole trap differs significantly from the harmonic one and deviations from the harmonic approximation might become relevant.

Evaporative cooling in optical traps is a simple and efficient method for reaching low enough temperatures to produce degenerate Bose [17] and Fermi [20] gases. The technique is based on the preferential removal of atoms with higher energy than the average energy. Subsequently, the remaining atoms thermalize through elastic collisions, which leads to a lower average energy and temperature. Our discussion here follows [32] which describes evaporation in a classical approximation. The latter is justified as typical temperatures are still much higher than the quantum level spacing of an atom in the trap potential. On the other hand the temperatures shall be low enough to work in the s-wave scattering regime with an energy independent cross section $\sigma = 8\pi a^2$, where a is the scattering length.

A central ambition is to determine the evolution of the energy distribution of a trapped gas during so-called plain evaporation [32]. Quite generally, well above the transition temperature, the trapped gas is well described by a classical phase-space distribution $f(\mathbf{r}, \mathbf{p})$, which is normalized according to

$$N = \frac{1}{(2\pi\hbar)^3} \int d^3r d^3p f(\mathbf{r}, \mathbf{p}). \quad (10)$$

The time evolution of $f(\mathbf{r}, \mathbf{p})$ is determined by the Boltzmann equation [33]

$$\left(\frac{\mathbf{p}}{m} \nabla_{\mathbf{r}} - \nabla_{\mathbf{r}} U \nabla_{\mathbf{p}} + \frac{\partial}{\partial t}\right) f(\mathbf{r}, \mathbf{p}) = \mathcal{I}(\mathbf{r}, \mathbf{p}), \quad (11)$$

with the collision integral \mathcal{I} for s-wave scattering and thus an energy-independent cross section σ given by

$$\mathcal{I}(\mathbf{r}, \mathbf{p}_4) = \frac{\sigma}{2\pi m (2\pi\hbar)^3} \int d^3p d\Omega' q \{f(\mathbf{r}, \mathbf{p}_1) f(\mathbf{r}, \mathbf{p}_2) - f(\mathbf{r}, \mathbf{p}_3) f(\mathbf{r}, \mathbf{p}_4)\}. \quad (12)$$

As in [32], \mathbf{p}_3 and \mathbf{p}_4 are the momenta of two atoms before the collision, $\mathbf{p}_1 = \mathbf{P}/2 + \mathbf{q}'$ and $\mathbf{p}_2 = \mathbf{P}/2 - \mathbf{q}'$ the momenta after the collision. Here we denote a relative momentum with $\mathbf{q} = (\mathbf{p}_3 - \mathbf{p}_4)/2$, the total momentum with $\mathbf{P} = \mathbf{p}_3 + \mathbf{p}_4$, and $|\mathbf{q}'| = |\mathbf{q}|$. Ω' denotes the direction of \mathbf{q}' with respect to \mathbf{q} .

The assumption of sufficient ergodicity leads to a phase space distribution as a function of the scaled single-particle energy ϵ only, such that it can be written as

$$f(\mathbf{r}, \mathbf{p}) = N \int d\epsilon \delta((U(\mathbf{r}) + p^2/2m)/U_0 - \epsilon) f(\epsilon), \quad (13)$$

where $f(\epsilon)$ is the distribution of atoms as a function

of scaled energy ϵ which we define to be normalized to one. The substitution (13) leads to a rigorous simplification of the Boltzmann equation (11). After applying $(2\pi\hbar)^{-3} \int d^3r d^3p \delta(U(\mathbf{r}) + p^2/2m - \epsilon)$ to both sides of (11), the gradient terms on the left-hand side sum to zero, and only a term $g(\epsilon)\partial f(\epsilon)/\partial t$ survives. The right hand side can also be simplified, as described in [32]. As a general result, the following kinetic equation for the time evolution of the distribution function $f(\epsilon)$ (initially normalized to one) of a gas in a trap with density of states $g(\epsilon)$ is obtained:

$$g(\epsilon_4)\dot{f}(\epsilon_4) = \int d\epsilon_1 d\epsilon_2 d\epsilon_3 \delta(\epsilon_1 + \epsilon_2 - \epsilon_3 - \epsilon_4) g(\min(\epsilon_1, \epsilon_2, \epsilon_3, \epsilon_4)) \{f(\epsilon_1)f(\epsilon_2) - f(\epsilon_3)f(\epsilon_4)\}. \quad (14)$$

Here, dot denotes time derivative $\dot{f} = \frac{df}{d\tau}$ with respect to a dimensionless time $\tau = N_0 \frac{m\sigma U_0^2}{\pi^2 \hbar^3} t$ where N_0 is the initial number of atoms. Recall that $f(\epsilon)$ is normalized to one initially. Its time evolution is obtained numerically by writing the integral as a sum over a discretized energy scale. In Figure 5 we show evaporation dynamics for dipole trap (top) and for the truncated harmonic potential (bottom). Furthermore, the evolution of the number density $g(\epsilon)f(\epsilon)$ is shown for the two potentials; its integral reflects the number of atoms remaining in the trap.

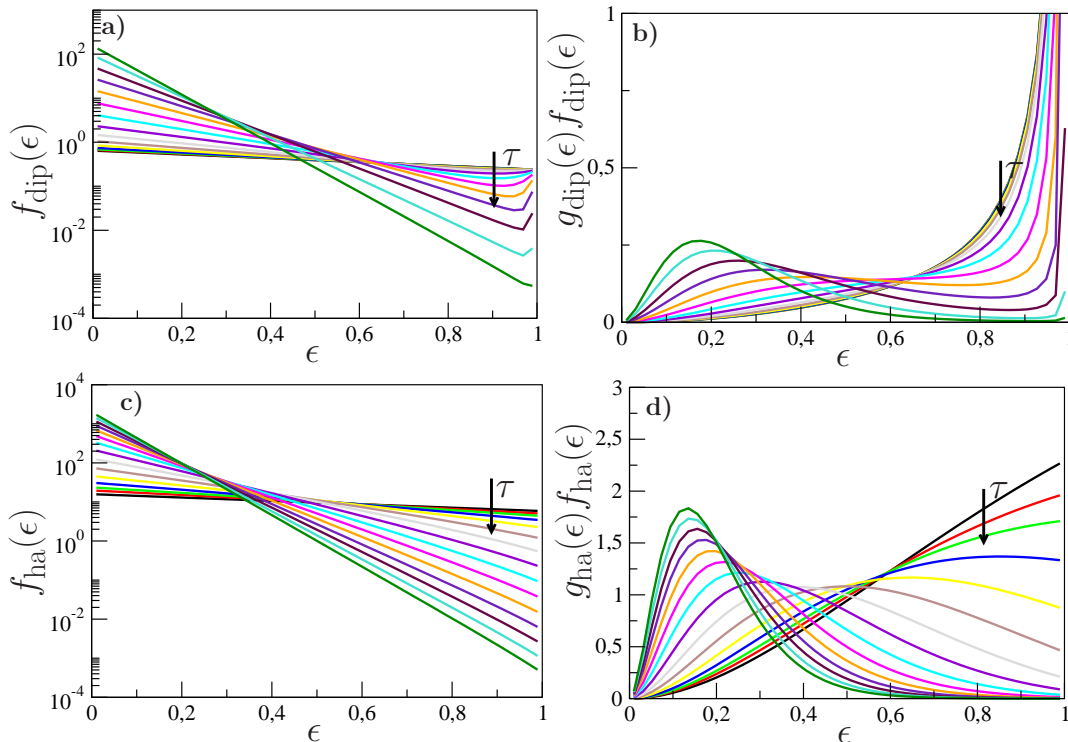


FIG. 5: Time evolution of normalized distribution function $f(\epsilon)$ during plain evaporative cooling in a dipole trap (a) and a harmonic trap (c); time evolution of the number density $g(\epsilon)f(\epsilon)$ for the dipole (b) and the harmonic trap (d). Initially, $f(\epsilon)$ is chosen to correspond to a Boltzmann distribution with $k_B T = U_0$, normalized to one. The arrows indicate increasing time; time steps grow exponentially.

We see from Figure 5 that for all times, $f(\epsilon)$ can well be

approximated by an exponential, i.e. a Boltzmann dis-

tribution. Apparently, during evaporation the thermal nature of the distribution is preserved. In the case of the dipole trap potential, it is only at the edge of the potential well that $f(\epsilon)$ differs somewhat from an exponential, due to the singularity in the density of states.

Being a Boltzmann distribution, the slope of the graphs allows us to extract a temperature of the atoms remaining in the trap.

Furthermore, as the graphs in Figure 5 a) and c) reveal, the rate of change of $f(\epsilon)$ for the dipole trap is smaller than for the harmonic potential. The same conclusion can be drawn from parts b) and d) of the same figure. As the integral over $g(\epsilon)f(\epsilon)$ equals the number of trapped atoms, one finds that the evaporation process in the truncated harmonic trap happens much faster than in the dipole trap. However, at the end of the evaporation less atoms are left in the dipole trap, while the final temperature is approximately the same.

In order to investigate these observations in more detail, we calculate the number of atoms remaining in the trap by integrating over the number density $g(\epsilon)f(\epsilon)$. Moreover, we determine the temperature of the remaining atoms by fitting a Boltzmann distribution to $f(\epsilon)$, as a function of time.

Before we discuss these results, however, we want to turn to the semianalytical solutions of equation (14), which are described in [32]. The starting point is the replacement of the exact energy distribution function by a truncated Boltzmann distribution, which we saw is pretty well justified by looking at Figure 5;

$$f(\epsilon, t) \approx a(t) \exp(-U_0\epsilon/k_B T(t)) \Theta(\epsilon_t - \epsilon). \quad (15)$$

The Heaviside step function ensures that $f(\epsilon, t) = 0$ for $\epsilon > \epsilon_t$; particles with an energy above threshold escape from the trap. It is worth mentioning that $T = T(t)$ is not a temperature in the strict thermodynamic sense, since evaporation is a nonequilibrium process; but it surely is a convenient parameter characterizing the essentially nonequilibrium distribution. For the sake of clarity we introduce the dimensionless “temperature” $\tilde{T} = k_B T/U_0$ and a scaled total internal energy $\tilde{E} = E/(U_0 N_0)$. We keep the single-particle energy ϵ scaled to U_0 as well.

Substituting the truncated Boltzmann distribution (15) in equation (14), the integration can be performed easily. In order to determine the rate of change of the number of trapped atoms one integrates over untrapped energy states with $\epsilon_4 = \epsilon_1 + \epsilon_2 - \epsilon_3 > \epsilon_t > \epsilon_1, \epsilon_2 > \epsilon_3$:

$$\dot{N}_{\text{ev}}/N_0 = - \int_{\epsilon_t}^{\infty} d\epsilon_4 g(\epsilon_4) \dot{f}(\epsilon_4) = -a^2 \tilde{T} e^{-\eta} V \quad (16)$$

with

$$V = \int_0^{\epsilon_t} d\epsilon g(\epsilon) \{ (\epsilon_t - \epsilon - \tilde{T}) e^{-\epsilon/\tilde{T}} + \tilde{T} e^{-\eta} \}, \quad (17)$$

which corresponds to the “effective volume for elastic collisions” of [32]. Note that the factor $a = a(\tau)$ in equ. (16)

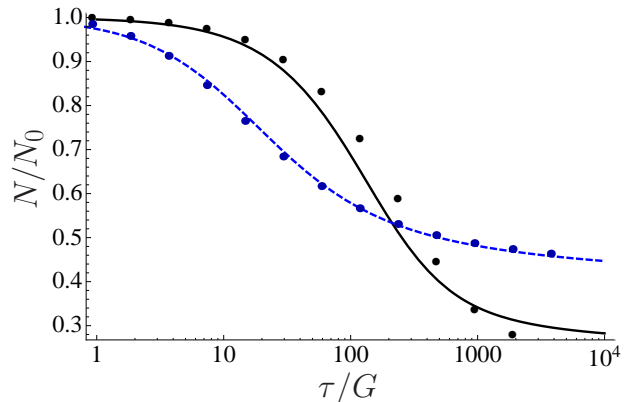


FIG. 6: Fraction of atoms N/N_0 remaining in the trap as a function of scaled time τ/G after starting evaporation from a scaled temperature $\tilde{T} = k_B T/U_0 = 1$. The black, solid line is the result for the dipole trap and the blue dashed for its harmonic approximation obtained by integration of the differential equations resulting from the truncated Boltzmann approximation. The squares and circles are the results from the fully numerical treatment for dipole and harmonic trap, respectively.

has to be determined from the normalization condition $a(\tau) = (N(\tau)/N_0) / \int_0^{\epsilon_t} d\epsilon g(\epsilon) e^{-\epsilon/\tilde{T}(\tau)}$.

The evaporation of atoms leads to a loss of internal energy of the trapped gas. Following the elaborations in [32], we find an evolution equation somewhat similar to (16) for the scaled total energy \tilde{E} . On the other hand, the rate of change of the internal energy due to the evaporation of atoms is

$$\dot{\tilde{E}} = C\dot{\tilde{T}} + \mu(\dot{N}/N_0) \quad (18)$$

where C denotes the heat capacity $C = (\partial\tilde{E}/\partial\tilde{T})_N$ and $\mu = (\partial\tilde{E}/\partial(N/N_0))_{\tilde{T}} = \tilde{E}/(N/N_0)$ a chemical potential. We thus arrive at coupled differential equations which describe the rate of change of temperature, atom number and internal energy during evaporation in closed form. These can be solved numerically.

Using this approximative set of differential equations, we want to investigate the evaporation process in the dipole trap based on the true density of states (5) and compare with results for the harmonic approximation. Furthermore, we compare with a full numerical treatment based on the Boltzmann equation (14). In Figure 6 we show the evolution of the number of remaining atoms and in Fig. 7 their temperature, respectively, during evaporation. We choose an initial scaled temperature of $\tilde{T} = k_B T/U_0 = 1$. Recall that time is dimensionless with $\tau = N_0 \frac{m\sigma U_0^2}{\pi^2 \hbar^3} t$ with N_0 the initial number of atoms in the trap (similar to [32], times are scaled to τ/G). The curves are obtained by solving the above mentioned coupled differential equations based on the truncated Boltzmann ap-

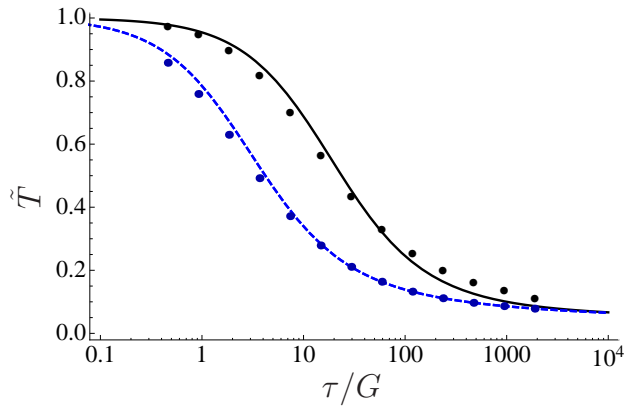


FIG. 7: Scaled temperature $\tilde{T} = k_B T/U_0$ of the remaining atoms as a function of scaled time τ/G after starting evaporation from a temperature $\tilde{T} = 1$. The black, solid line is the result for the dipole trap and the blue dashed line for its harmonic approximation obtained by integration of the differential equations resulting from the truncated Boltzmann approximation. The squares and circles result from the fully numerical treatment for dipole and harmonic trap, respectively.

proximation, while the symbols follow from the numerical solution of equ. (14), by integrating over $g(\epsilon)f(\epsilon)$ for the number of atoms and by fitting an exponential to $f(\epsilon)$ to determine the temperature.

Figures 6 and 7 confirm that the evaporation process in the dipole trap is indeed much slower than in a harmonic trap as already indicated in Figure 5. The harmonic approximation may lead to predictions that differ by more than an order of magnitude. Furthermore, we see that in a dipole trap, more atoms get lost eventually compared to the harmonic trap. The final temperature, on the other hand, turns out to be pretty much the same.

In the case of the dipole trap the truncated Boltzmann approximation does not describe the distribution function $f(\epsilon)$ accurately over the whole energy range. Clearly, we see deviations for energies near the threshold in Figure 5. These explain the differences between the numerical and the approximative results for atom number and temperature in Figures 6 and 7.

V. A BOSE-EINSTEIN CONDENSATE IN A SINGLE-BEAM DIPOLE TRAP

We here assume that a Bose-Einstein condensate has been created in or transferred to a single-beam optical dipole trap. At temperatures well below the critical temperature, the condensate wave function is well described by the mean field Gross-Pitaevskii equation

$$\left(-\frac{\hbar^2}{2m}\Delta + U(\mathbf{r})\right)\psi(\mathbf{r}) + g|\psi(\mathbf{r})|^2\psi(\mathbf{r}) = \mu\psi(\mathbf{r}) \quad (19)$$

with μ the chemical potential. Often, the so-called Thomas-Fermi approximation may be employed [4, 5] which describes the BEC in the limit of large atom numbers such that the contribution of the kinetic energy may be neglected with respect to the internal energy and the potential energy. The condensate wave function is then given by the simple formula

$$|\psi(\mathbf{r})|^2 = \frac{\mu - U(\mathbf{r})}{g}, \quad (20)$$

valid for all positions \mathbf{r} such that the right hand side is positive, and $\psi(\mathbf{r}) = \mathbf{0}$ otherwise. The parameter g describes the strength of the atom-atom interaction and is connected to the s-wave scattering length a through $g = 4\pi\hbar^2 a/m$. For a harmonic approximation, the Thomas-Fermi wave function (20) leads to the analytical expression $\mu = (15gN/4\pi w_0^2 z_0 U_0)^{2/5}$ for the chemical potential, where μ is normalized to U_0 and positive (similar to ϵ). Remarkably, in Thomas-Fermi approximation, even the full dipole potential (1) allows for an analytical treatment. By integrating expression (20) over \mathbf{r} and equating it with the total atom number N we find the simple expression

$$N(\mu) = \frac{4\pi}{9g} z_0 w_0^2 U_0 \left(\sqrt{\frac{\mu}{1-\mu}} (4\mu - 3) - 3(\mu - 1) \arctan\left(\sqrt{\frac{\mu}{1-\mu}}\right) \right). \quad (21)$$

Similar to the density of states (5), the number of particles N as a function of the chemical potential μ develops a singularity at $\mu = 1$ in the dipole trap. Clearly, in the harmonic trap the particle number for any μ remains finite. For small condensate numbers N the chemical potentials agree, as shown in Figure 8.

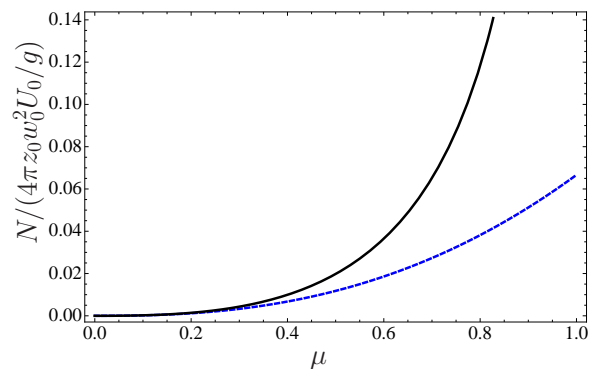


FIG. 8: Chemical potential versus atom number of a condensate in a dipole trap (black, solid) and a harmonic trap (blue, dashed) in Thomas-Fermi approximation.

Furthermore, we found an analytical expression for the internal (interaction) energy in Thomas-Fermi approximation for a condensate. By integrating the squared

expression (20), one finds for the harmonic approximation the well-known $E_{\text{int}}(N) = \frac{2}{7}U_0 \left(\frac{15g}{4\pi z_0 w_0^2 U_0}\right)^{2/5} N^{7/5}$, while for the dipole trap the result can only be given analytically as a function of the chemical potential:

$$E_{\text{int}}(\mu) = \frac{\pi z_0 w_0^2 U_0^2}{4g} \left(\sqrt{\frac{\mu}{1-\mu}} \left(\frac{23}{9}(\mu-1) + \frac{38}{9}(\mu-1)^2 \right) + \left(1 - \frac{8}{3}(\mu-1)^2\right) \arctan \left(\sqrt{\frac{\mu}{1-\mu}} \right) \right). \quad (22)$$

Clearly, the internal energy remains finite for any finite number of atoms.

Finally, we determine the Thomas-Fermi radii of the condensate in such an optical dipole trap. They are defined by means of the condition $U(\mathbf{r}) = \mu$ and characterize the extensions of the condensate in the various directions. For the harmonic potential they are well known to be $R_\rho(\mu) = \frac{w_0}{\sqrt{2}}\sqrt{\mu}$ and $R_z(\mu) = z_0\sqrt{\mu}$. For the dipole trap, we find easily

$$R_\rho(\mu) = \frac{w_0}{\sqrt{2}}\sqrt{-\ln(1-\mu)} \quad ; \quad R_z(\mu) = z_0\sqrt{\frac{\mu}{1-\mu}}. \quad (23)$$

Clearly, as $\mu \rightarrow 0$, these expressions coincide with the harmonic case. In general, however, in particular along the z-axis (direction of propagation of the laser), the Thomas-Fermi radius in the dipole trap differs strongly from the one obtained in the harmonic trap for large μ . Both expressions diverge for $\mu \rightarrow 1$. In Figure 9 we show $R_z(\mu)$ for both traps.

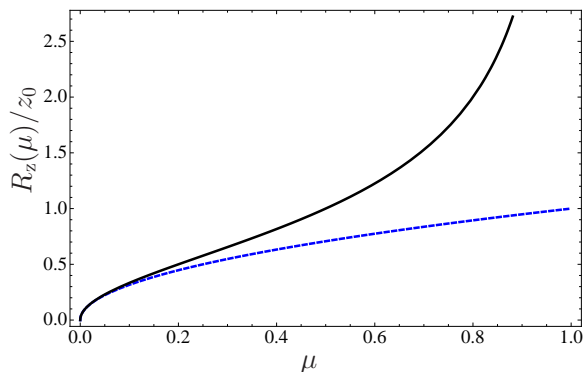


FIG. 9: Thomas-Fermi radius along the propagation direction of the laser versus chemical potential for dipole trap (black, solid) and its harmonic approximation (blue, dashed).

It should be emphasized that temperatures and atom numbers that may be achieved with evaporative cool-

ing as described in the first part of this paper lead to “small” condensates that may well be described with the harmonic approximation. Nevertheless, it is conceivable that much larger condensates are created in some other trap before being loaded into a single-beam optical dipole trap such that deviations from the harmonic trap become relevant and our results apply.

VI. CONCLUSION

We found an analytical expression for the density of states of an optical dipole trap potential, consisting of one single focused laser beam. The density of states has a singularity at the potential edge of the trap.

Without further consideration, this singularity would prevent Bose-Einstein condensation from occurring. However, since an effective cutoff will be present in current-day experiments (e.g. due to gravity), condensation can be achieved. Then, near condensation, the usual harmonic approximation is valid and may be used to determine, e.g., the critical temperature for Bose-Einstein condensation.

Still, the existence of this singularity makes itself felt whenever states of higher energy are involved as, for instance, in evaporative cooling. We found that plain evaporative cooling is much slower (about one order of magnitude) in the dipole trap compared to its harmonic approximation. In addition, for the optical dipole trap more atoms get lost on the way to the same temperature compared to the harmonic trap.

Finally, we determine analytical expressions for chemical potential, internal energy and Thomas-Fermi radii for the true optical dipole trap in Thomas-Fermi approximation. It turns out that the chemical potential and the radii of the condensate develop singularities similar to the density of states.

While we here concentrate on bosonic gases, it will be interesting to see how the semiclassical expression (5) will be of relevance for the behavior of fermionic gases in single-beam dipole traps.

Acknowledgments

This work came into being due to many fruitful discussions we shared with Hanspeter Helm and his co-workers in Freiburg, in particular Christoph Käfer. L. S. acknowledges support from the International Max Planck Research School (IMPRS), Dresden.

[1] M. H. Anderson, J. R. Ensher, M. R. Matthews, C. E. Wieman, and E. A. Cornell, *Science* **269**, 198 (1995).

[2] K. B. Davis, M.-O. Mewes, M. R. Andrews, N. J. van Druten, D. S. Durfee, D. M. Kurn, and W. Ketterle, *Phys. Rev. Lett.* **75**, 3969 (1995).

- [3] C. C. Bradley, C. A. Sackett, J. J. Tollett, and R. G. Hulet, *Phys. Rev. Lett.* **75**, 1687 (1995).
- [4] C. J. Pethick and H. Smith, *Bose-Einstein Condensation In Dilute Gases* (Cambridge University Press, Cambridge, 2002).
- [5] L. Pitaevskii and S. Stringari, *Bose-Einstein Condensation* (Oxford University Press, Oxford, 2003).
- [6] I. Bloch, J. Dalibard, and W. Zwerger, *Rev. Mod. Phys.* **80**, 885 (2008).
- [7] C. E. Wieman, and E. A. Cornell, *Rev. Mod. Phys.* **74**, 875 (2002).
- [8] W. Ketterle, *Rev. Mod. Phys.* **74**, 1131 (2002).
- [9] S. Stellmer, Me.K. Tey, B. Huang, R. Grimm, and F. Schreck, *Phys. Rev. Lett.* **103**, 200401 (2009).
- [10] Y. N. Martinez de Escobar, P. G. Mickelson, M. Yan, B. J. DeSalvo, S. B. Nagel, and T. C. Killian, *Phys. Rev. Lett.* **103**, 200402 (2009).
- [11] T. Takekoshi, and R. J. Knize, *Opt. Lett.* **21**, 77 (1996).
- [12] S. Friebel, C. D'Andrea, J. Walz, M. Weitz, and T. W. Hänsch, *Phys. Rev. A* **57**, R20 (1998).
- [13] C. S. Adams, H. Jin Lee, N. Davidson, M. Kasevich, and S. Chu, *Phys. Rev. Lett.* **74**, 3577 (1995).
- [14] A. J. Kerman, V. Vuletić, C. Chin, and S. Chu, *Phys. Rev. Lett.* **84**, 439 (2000).
- [15] D. -J. Han, S. Wolf, S. Oliver, C. McCormick, M. T. DePue, and D. S. Weiss, *Phys. Rev. Lett.* **85**, 724 (2000).
- [16] T. Ido, Y. Isoya, and H. Katori, *Phys. Rev. A* **61**, 061403 (2000).
- [17] M. D. Barrett, J. A. Sauer, and M. S. Chapman, *Phys. Rev. Lett.* **87**, 010404 (2001).
- [18] T. Weber, J. Herbig, M. Mark, H. -C. Nägerl, and R. Grimm, *Science* **299**, 232 (2003).
- [19] Y. Takasu, K. Maki, K. Komori, T. Takano, K. Honda, M. Kumakura, T. Yabuzaki, and Y. Takahashi, *Phys. Rev. Lett.* **91**, 040404 (2003).
- [20] S. R. Granade, M. E. Gehm, K. M. O'Hara, and J. E. Thomas, *Phys. Rev. Lett.* **88**, 120405 (2002).
- [21] L. Luo, B. Clancy, J. Joseph, J. Kinast, A. Turlapov, and J. E. Thomas, *New J. Phys.* **8**, 213 (2006).
- [22] G. Cennini, G. Ritt, C. Geckeler, and M. Weitz, *Appl. Phys. B* **77**, 773 (2003).
- [23] C. Käfer, R. Bourouis, J. Eurisch, A. Tripathi, and H. Helm, *Phys. Rev. A* **80**, 023409 (2009).
- [24] A. Szczepkowicz, L. Krzemień, A. Wojciechowski, K. Brzozowski, M. Krüger, M. Zawada, M. Witkowski, J. Zachorowski, and W. Gawlik, *Phys. Rev. A* **79**, 013408 (2009).
- [25] C. Y. Yang, P. Halder, O. Appel, D. Hansen, and A. Hemmerich, *Phys. Rev. A* **76**, 033418 (2007).
- [26] J. J. Thorn, E. A. Schoene, T. Li, and D. A. Steck, *Phys. Rev. Lett.* **100**, 240407 (2008).
- [27] F. Fang, H. Wang, D. Feldbaum, D. J. Vieira, and X. Zhao, *Phys. Rev. A* **79**, 043406 (2009).
- [28] S. Balik, A. L. Win, and M. D. Havey, *Phys. Rev. A* **80**, 023404 (2009).
- [29] P. Meystre and M. Sargent III, *Elements of Quantum Optics* (Springer Verlag, 1999).
- [30] M. Abramowitz and I. A. Stegun, *Handbook of Mathematical Functions with Formulas, Graphs, and Mathematical Tables* (Dover Publications, 1964).
- [31] V. Bagnato, D. E. Pritchard, and D. Kleppner, *Phys. Rev. A* **35**, 4354 (1987).
- [32] O. J. Luiten, M. W. Reynolds, and J. T. M. Walraven, *Phys. Rev. A* **53**, 381 (1996).
- [33] K. Huang, *Statistical Mechanics*, (Wiley, New York, 1963).